SUBMERGED SELF-PROPULSION DRIVEN BY THE LEIDENFROST EFFECT

Adrian Jonas[1,*], Daniel Orejon[1], Khellil Sefiane[1]

[1]Institute for Multiscale Thermofluids, School of Engineering, University of Edinburgh, Edinburgh, EH9 3JL, United Kingdom

ABSTRACT

This paper presents experimental investigations of submerged self-propulsion due to the Leidenfrost effect. Cylinders, first heated in an oven, are removed and released into a vertical column filled with Novec 7000. The experiments investigate five different topological designs, and bored-out hollows force vertical free-fall. The control is a smooth cylinder, while the others have ratchet teeth engraved on their surface. Ratcheted cylinders are manufactured in pairs to compare ratchet directionality. One has ratchets facing the direction of the fall (FD), and the other faces the trailing end (FU). Comparing two aspect ratios, 2.2 and 11.4, against a smooth control gives insights into viscous drag force contributions. The falling trajectories are filmed using a high-speed camera and physical characteristics are extracted. A highly accurate tracking tool (Moxie Analyser) reduced experimental error and measurement noise. Repeated experiments determine the instability of any given experimental run. Cylinders initially heated to 550^{o}C present highly inaccurate while repeat-ability increases as initial temperature decreases. Interestingly, the time taken to reach terminal velocity increases with initial temperature while terminal velocity decreases, respectively. The depth at which terminal velocity occurs also decreases with increasing initial temperature. Inconclusive evidence suggests the existence of submerged self-propulsion when comparing ratcheted cylinders. Vapour produced from boiling dominates a free-fall, ultimately reducing the terminal velocity regardless of cylinder topography. Barriers in determining vapour volume and drag coefficients of superheated free-falling objects limit the application of the data presented herein.

1 INTRODUCTION

In 1756, Johann Gottlob Leidenfrost extensively studied the levitation of droplets on hot surfaces [1]. Centuries later, Linke *et al.* demonstrated that liquid droplets could propel themselves on ratcheted surfaces when heated above the Leidenfrost point [2]. Numerical [3], and analytical models [4] corroborated with experimental observations [5] show that the asymmetry of a substrate rectifies the vapour flow exiting in a specific direction. Self-propulsion of evaporating liquids and sublimating solids occurs then on various textured substrates such as ratchets [6], herringbones [7], and asymmetric nanostructures [8]. Wells *et al.* demonstrated dry ice rotation on turbine-like substrates [9], and subsequently, sustained rotation of droplets has produced net torque [10]. Beyond droplets, supercavitation attracts interest. In 1977, the Soviet Navy introduced the Shkval torpedo, a supercavitating weapon that travelled through a body of water at more than 100 ms^{-1} due to a reduction in surface friction [11]. More recently, Vakarelski *et al.* showed that at lower speeds, the Leidenfrost effect also shows drag-reducing characteristics for superheated spheres suggesting the vapour layer reduces flow separation [12]. Combining a continuous and lubricating vapour layer with the self-propelling nature of ratchets could prove to change the way we think about drag reduction. Rather than view the problem of drag reduction as simply reducing either, the flow separation or the surface area in contact with the fluid, we propose that drag may be reduced by rectifying flow around an object in the direction of motion. When a droplet boils atop a solid surface in the Leidenfrost regime, the fluid is levitated above the surface with evaporated fluid expulsion. This expulsion of vapour can be directed with asymmetric shapes such as ratchets to produce microflows that drive the droplet. The direction of motion follows the direction of vapour flow, where it is speculated that the propelling mechanism is that of viscous drag. We aim to exploit the propulsion mechanism to increase the speed of travelling objects immersed in a fluid additionally to decreasing drag.

*Corresponding author: s1521326@sms.ed.ac.uk

2 EXPERIMENTAL

Table 1: Dimensions of cylinder design used within this experimental investigation.

Description	D, mm	d, mm	L, mm	x, mm	P, mm	h, mm	w, mm	h/w
Control	10	8.5	40	27	3	N/A	0	N/A
FU/FD 2.2	10	8.5	40	27	3	1.1	0.5	2.2
FU/FD 11.4	10	8.5	40	27	3	5.7	0.5	11.4

Lagubeau *et al.* reported the self-propelling viscous drag force to be in the order of μN [13]. Therefore, ratchets engraved along the length of the cylinders would maximise the chances of observing self-propulsion. Unfortunately, Chu *et al.* found that free-falling uniform cylinders tend to orientate themselves horizontally; however, reported that a cylinder will fall vertically by separating the centre of mass (CoM) from the centre of volume (CoV) [14]. Given the range of temperatures our experiments occur at, the obvious choice was to hollow the cylinders out. An analysis of the drag forces on either side of the centre of gravity (CoG) gave us the confidence that a cylinder with a hollow 62.5% its length and 85% its diameter (Table 1) will cause a cylinder to fall vertically in a moderately dense fluid. In hollowing the cylinders, we also reduce the energy any given cylinder can store. To maximise the probability of achieving the Leidenfrost effect for a sufficient period for a cylinder to reach terminal velocity, we chose aluminium, which has a significantly high specific heat capacity among common metals. Manufacturing ratchets into aluminium cylinders at this scale is technically tricky, resulting in imperfect ratchet structures, especially for ratchets with an aspect ratio of 2.2. The experiment itself consisted of first heating cylinders in an oven before removing them by hand and releasing them to fall into the column (Table 1). With aluminium's melting point at $\approx 600^{o}$C, our experimental temperature maximum was limited to 550^{o}C to avoid any unintentional tampering of the ratchet structures. A guiding release shoot ensured true free-fall occurred only once the cylinders were submerged (Figure 1). A wide-angle lens was employed to capture as much of the cylinders' fall as possible. Wide-angle lenses are subject to distort images near the edges of image capture. Our results herein presented will mostly consider the information at terminal velocity. Preliminary experiments showed that terminal velocity, across all temperatures, occurs at a depth of 0.5m. Therefore, the centre of image capture occurs at a depth of 0.5m (Figure 2).

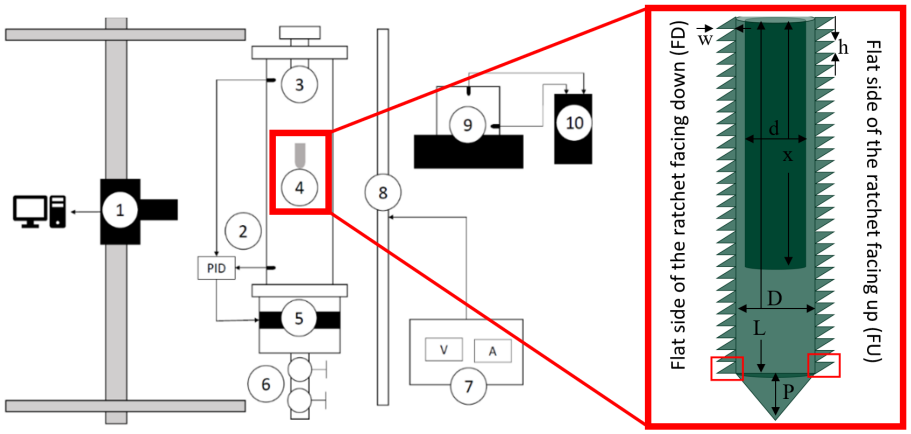

Figure 1: Experimental Schematic. (1)-Chronos 2.1 HSC. (2)-Temperature Control. (3)-Guiding Release Shoot. (4)-Cylinder. (5)-Heater. (6)-Extraction Unit. (7)-Power Supply. (8)-Strip Light. (9)-Oven. (10)-Controller.

3 METHODOLOGY

Existing software which could process the high-speed camera (HSC) footage led to significant errors and experimental noise. Therefore, we present a bespoke software tool (Moxie Analyser) that can find a moving object within a video, track its position, and calculate physical parameters such as velocity and acceleration. Figure 2 shows the initial (subfigure 2a) and final (subfigure 2b) frames used to calibrate the Moxie Analyser for a free-falling smooth cylinder heated to 550^{o}C. The Moxie Analyser requires the experimentalist to insert spacial measurements used as calibration points to convert pixels to distance values. The frame rate defines the experiment's time acquisition, and important physical parameters are calculated with distance-time relations. An HSC decreases the time between each data acquisition, increasing the accuracy of the calculated parameters. The tracking tool also produces a processed image (subfigure 2d) from the original captured footage (subfigure 2c), which shows the experimentalist the free-fall trajectory and provisional vapour layer thickness. The noise reduction procedure of the data produced by the tracking tool is displayed. Raw data overlapped by data produced from a robust quadratic regression algorithm built within MATLAB removes noise from the results. Points extracted at equal intervals of time, plotted in subfigures (2e) and (2f), shows the output of the noise reduction algorithm. Experimental iterations identify random errors. Subfigures (2e) and (2f) presents the extracted data from 5 iterations of the experiment at isothermal conditions. Subfigure (2e) shows errors in velocity across experimental iterations, while subfigure (2f) shows errors in depth. The time error comes from the frame rate used to capture the data. Preliminary experiments determined that at terminal velocity, film boiling occurs for cylinders initially heated to temperatures to 350^{o}C and beyond, nucleate boiling occurs for cylinders initially heated to temperatures to 150^{o}C and beyond, and single-phase free-fall is observed for cylinders initially heated to 50^{o}C and below.

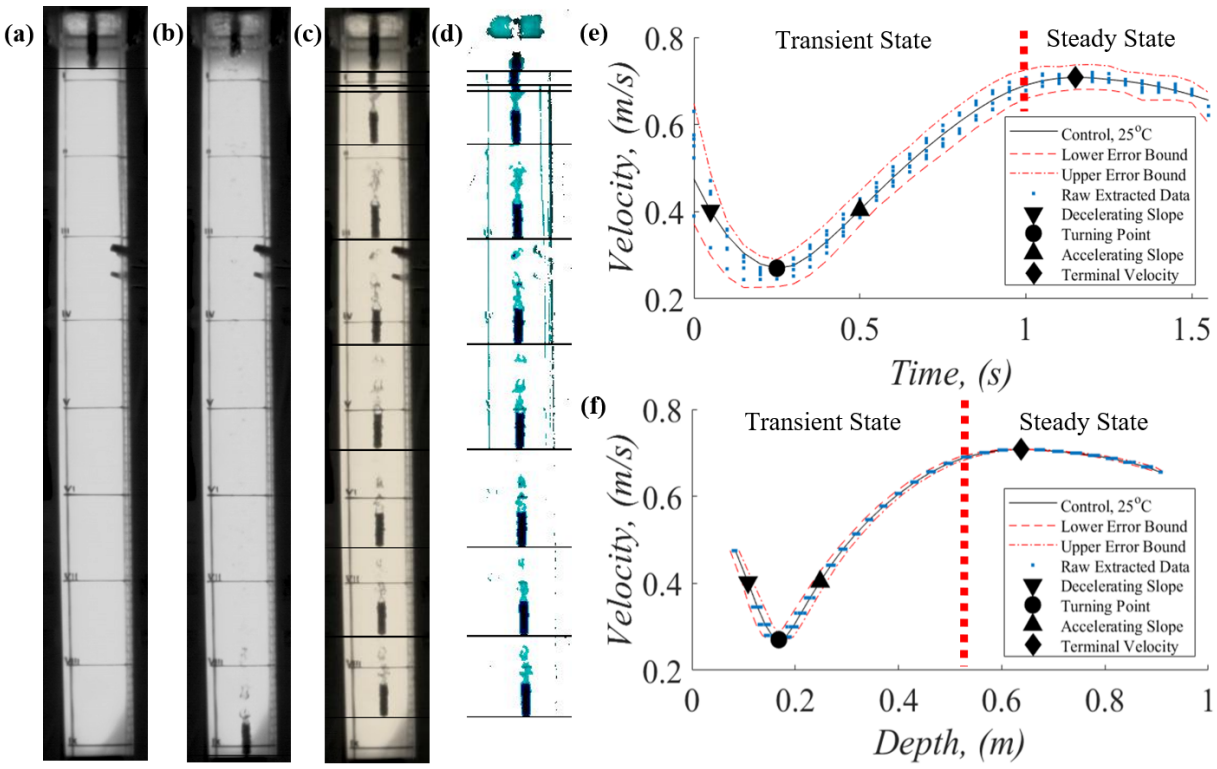

Figure 2: Initial frame (a), final frame (b), and trajectory (c-d) for a smooth cylinder heated to 550^{o}C. Graphical representation of random error in velocity (d) and depth (e) for a smooth cylinder falling in isothermal conditions.

4 RESULTS

Here we present our results in boiling regimes and ratchet aspect ratio categories. Control runs are duplicated across aspect ratios within figure 3. The transient state initially consists of a decelerating period. Each decelerating period comes before a turning point after which a cylinder begins to accelerate. The first plateau following the acceleration stage is determined to be the terminal velocity of the cylinder, and a steady-state condition is assumed henceforth. 25^oC represents isothermal conditions. Though the boiling point of Novec 7000 is 36^oC, runs at 50^oC and below presented as single-phase experiments following an analysis of the high-speed footage captured during the experiment. (subfigures 3 e-f). Further visual inspection determined the nucleate boiling regime of the experiments (subfigures 3 c-d). The nucleate boiling regime presents a highly unstable free-fall, so much in fact, that for AR 2.2 FU, no experiments within the constraints of our setup were able to complete the fall without touching the walls of the column. Film boiling presents increased uncertainty though more stable free-falls occurs as compared against the nucleate boiling regime (subfigures 3 a-b). AR 2.2 FD reaches terminal velocities of 0.44 ± 0.03 ms^{-1}, 0.38 ± 0.02 ms^{-1}, and 0.37 ± 0.06 ms^{-1} at initial temperatures of 350^oC, 450^oC, and 550^oC respectively (subfigures 4 e-f). Comparatively, AR 2.2 FU plateaus at 0.43 ± 0.03 ms^{-1}, 0.40 ± 0.04 ms^{-1}, and 0.33 ± 0.17 ms^{-1}. AR 11.4, FD gives 0.42 ± 0.05 ms^{-1}, 0.34 ± 0.06 ms^{-1}, and 0.33 ± 0.12 ms^{-1}, while FU presents with 0.41 ± 0.03 ms^{-1}, 0.37 ± 0.06 ms^{-1}, and 0.28 ± 0.04 ms^{-1}. Smooth cylinders fall with a similar trajectory to that observed with AR 2.2 FD, reaching terminal velocities of 0.40 ± 0.04 ms^{-1}, 0.37 ± 0.05 ms^{-1}, and 0.27 ± 0.11 ms^{-1}. AR 2.2 FU cylinders reach terminal velocity significantly sooner in comparison. For AR 11.4, we see less significance between ratchet directionality, with both cylinder's reaching terminal velocity before the smooth control.

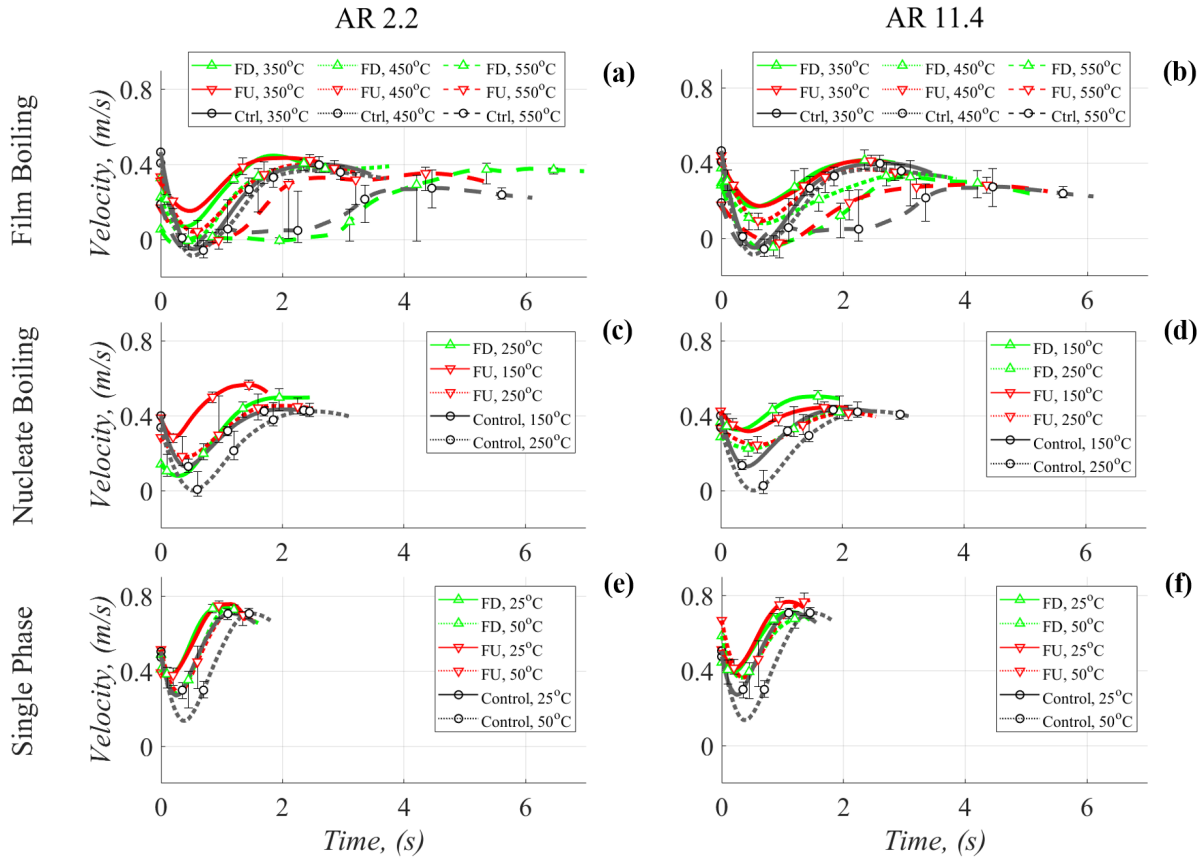

Figure 3: Velocity profiles of cylinders falling within film boiling, nucleate boiling, and single phase regimes.

5 DISCUSSION AND ANALYSIS

Considering only a smooth cylinder, the terminal velocity decreases with increasing initial temperature. Conversely, time taken to reach terminal velocity decreases with increasing initial temperature from 1.15s at 25^{o}C to 3.95s at 550^{o}C (subfigures 4 a-b). The depth at which terminal velocity occurs also decreases from 0.64±0.01m to 0.49±0.25m respectively (subfigures 4 c-d). When considering experiments within the Leidenfrost regime, we compare cylinders with equivalent surface area. For ratcheted cylinders falling with an initial temperature of 350^{o}C, we see no considerable difference in the terminal velocity measured between FD and FU cylinders with aspect ratios at both 2.2 and 11.4. The time to reach terminal velocity is 1.85s and 2.05s for AR 2.2 FD and AR 2.2 FU, respectively. For AR 11.4, the time taken is 2.35s for FD and FU. When initially heated to 450^{o}C, we observe a consistent ratchet directional dependency for both aspect ratios. FD cylinders fall slower than FU cylinders. Furthermore, FD cylinders take longer to reach their terminal velocity, with 3.00s for AR 2.2 FD and 2.36s for AR 2.2 FU. For AR 11.4, the time taken is 3.15s for FD and 2.35s for FU. For cylinders initially heated to 550^{o}C, we observe the opposite directional dependency. In this case, FD cylinders fall faster than FU cylinders; however, here, AR 2.2 FD (5.31s) takes longer to reach terminal velocity than AR 2,2 FU (2.65s) as opposed to AR11.4 FD (3.05s), which reaches its terminal velocity before AR 11.4 FU (4.05s). The longer a cylinder takes to reach terminal velocity, the cooler it is at the measurement point, thus the thinner the vapour layer. A thinner vapour layer should decrease the drag coefficient and buoyancy force

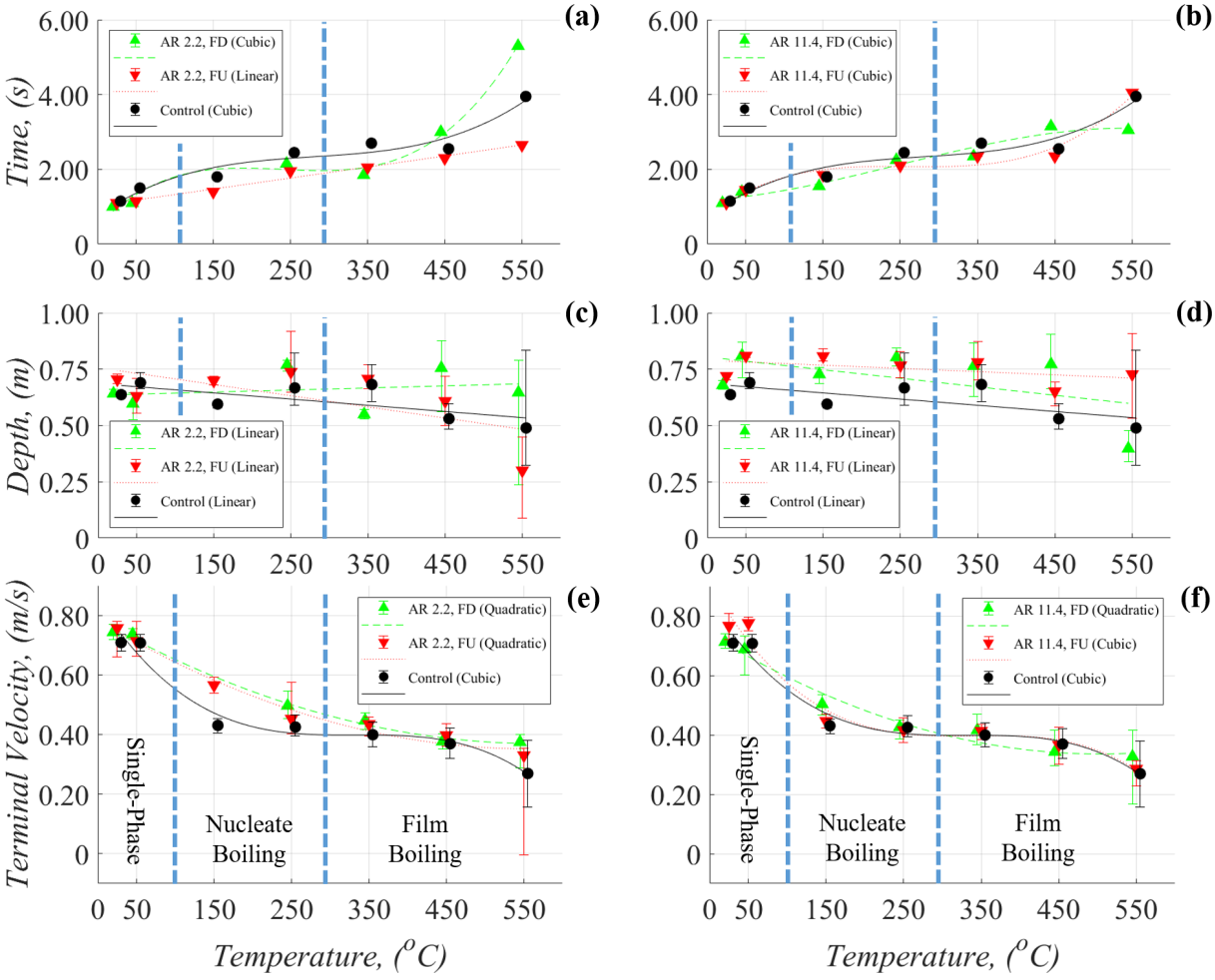

Figure 4: Time, depth, and corresponding terminal velocity of falling cylinders plotted against initial temperature.

and increase the viscous drag force. Our results present an interesting situation whereby ratcheted cylinders, initially heated to 450^oC, with FD topography, fall slower than their FU counterparts even when the forces opposing free-fall in the FD experiments are lesser than the FU experiments. One cannot point towards observations of ratchet self-propulsion because the self-propelling force for FD cylinders would be in the direction of the fall. A more intuitive result comes when a cylinder is initially heated to 550^oC, as here, an FD topography yields a faster falling cylinder. Furthermore, with an aspect ratio of 2.2, we see that the FD cylinder takes longer than an FU cylinder to reach its respective terminal velocity, while an aspect ratio of 11.4 yields the opposite result. A theoretical force balance would suggest the presence of self-propelling viscous drag forces for ratcheted cylinders initially heated to 550^oC.

6 CONCLUSION

Experiments investigating the free-fall of five cylinders boiling beyond the Leidenfrost point with varying topographies show ratchet directional dependency. Hollow aluminium cylinders with lengths of 40mm, diameters of 10mm, and hollows 50% V/V present with a sustained vapour film if heated to 350^oC and beyond. Increasing the vapour film around ratcheted cylinders increases the likelihood of observing self-propulsion due to viscous drag within a submerged environment. Results herein are inconclusive due to the significant uncertainty arising from falling cylinders while boiling in the Leidenfrost regime.

ACKNOWLEDGEMENTS

This work was supported by the UK Engineering and Physical Sciences Research Council (EPSRC) for the University of Edinburgh Centre for Doctoral Training. The experimental apparatus was largely built by the technicians at the University of Edinburgh, in particular, Mr S. Cummings, Mr P. Aitken, and Mr J. Graham. The aluminium cylinders used for the results presented herein were produced by George Brown & Sons Engineers Ltd.

REFERENCES

[1] J. G. Leidenfrost. On the fixation of water in diverse fire. *International Journal of Heat and Mass Transfer*, **9** (1966) 1153–1166.

[2] H. Linke, B. J. Alemán, L. D. Melling, M. J. Taormina, M. J. Francis, C. C. Dow-Hygelund, V. Narayanan, R. P. Taylor, & A. Stout. Self-propelled leidenfrost droplets. *Physical Review Letters*, **96** (2006) 2–5.

[3] T. R. Cousins, R. E. Goldstein, J. W. Jaworski, & A. I. Pesci. A ratchet trap for Leidenfrost drops. *Journal of Fluid Mechanics*, **696** (2012) 215–227.

[4] G. Dupeux, M. Le Merrer, G. Lagubeau, C. Clanet, S. Hardt, & D. Quéré. Viscous mechanism for Leidenfrost propulsion on a ratchet. *Epl*, **96**.

[5] G. Dupeux, T. Baier, V. Bacot, S. Hardt, C. Clanet, & D. Quéré. Self-propelling uneven Leidenfrost solids. *Physics of Fluids*, **25** (2013) 1–7.

[6] R. L. Agapov, J. B. Boreyko, D. P. Briggs, B. R. Srijanto, S. T. Retterer, C. P. Collier, & N. V. Lavrik. Asymmetric wettability of nanostructures directs Leidenfrost droplets. *ACS Nano*, **8** (2014) 860–867.

[7] D. Soto, G. Lagubeau, C. Clanet, & D. Quéré. Surfing on a herringbone. *Physical Review Fluids*, **1** (2016) 1–10.

[8] R. L. Agapov, J. B. Boreyko, D. P. Briggs, B. R. Srijanto, S. T. Retterer, C. P. Collier, & N. V. Lavrik. Length scale of Leidenfrost ratchet switches droplet directionality. *Nanoscale*, **6** (2014) 9293–9299.

[9] G. G. Wells, R. Ledesma-Aguilar, G. McHale, & K. Sefiane. A sublimation heat engine. *Nature Communications*, **6** (2015) 1–7.

[10] P. Agrawal, G. G. Wells, R. Ledesma-Aguilar, G. McHale, A. Buchoux, A. Stokes, & K. Sefiane. Leidenfrost heat engine: Sustained rotation of levitating rotors on turbine-inspired substrates. *Applied Energy*, **240** (2019) 399–408.

[11] S. Ashley. Warp Drive Underwater. *Scientific American*, **284** (2001) 70–79.

[12] I. U. Vakarelski, J. O. Marston, D. Y. Chan, & S. T. Thoroddsen. Drag reduction by leidenfrost vapor layers. *Physical Review Letters*, **106** (2011) 3–6.

[13] G. Lagubeau, M. Le Merrer, C. Clanet, & D. Quéré. Leidenfrost on a ratchet. *Nature Physics*, **7** (2011) 395–398.

[14] P. C. Chu, A. Gilles, & C. Fan. Experiment of falling cylinder through the water column. *Experimental Thermal and Fluid Science*, **29** (2005) 555–568.